

ELASTIC FIELDS DUE TO EIGENSTRAINS PART II: INCLUSION IN AN ISOTROPIC HALF-SPACE

SPINU Sergiu, GRADINARU Dorin

University "Stefan cel Mare" of Suceava, Faculty of Mechanical Engineering,
Mechatronics and Management, Romania
sergiu.spinu@fim.usv.ro, gradinaru@fim.usv.ro

Keywords: numerical simulation, inclusion problem, boundary condition, thermoelastic strains

Abstract: A fast algorithm to solve the inclusion problem for arbitrarily shaped eigenstrains is proposed and verified in this paper. A problem decomposition originally suggested by Chiu is employed. A solution to inclusion problem in infinite space was advanced in a companion paper. Pressure-free boundary condition is imposed with the aid of Boussinesq formulas and superposition principle, resulting in increased computational efficiency. Predictions for elastic fields due to a spherical inclusion are compared with existing analytical and/or numerical results, and a good agreement is found. The method appears well adapted for elastic-plastic contact modeling.

1. INTRODUCTION

An improved algorithm to assess stresses due to arbitrarily shaped eigenstrains in elastic isotropic half-space is advanced in a companion paper. Problem discretization is based on the existence of a solution for the influence coefficient, namely the linear elastic stress field induced in an isotropic half-space by a cuboid of uniform eigenstrains.

The first exact solution to this problem, advanced by Chiu, [2], is based on the summation of infinite space solutions of two mirror-image cuboids, which leaves the half-space boundary free of (shear) tractions, and the solution for the half-space subjected to pressure, which is employed to simulate the pressure-free surface condition. Jacq et al. [3] implemented this solution in an elastic-plastic three-dimensional semi-analytical code, and applied a two dimensional (2D) fast Fourier transform (FFT) algorithm to speed up the summation.

An alternative, direct approach to this problem was advanced by Liu and Wang [5]. Their analytical solution for the influence coefficients is based on Mindlin and Cheng's results, [7], and involves derivatives of four key integrals, resulting in increased model complexity. The algorithm advanced in this paper employs a simplified approach to impose the pressure-free surface condition, based on the assumption that spurious normal tractions corresponding to infinite space solution vanish outside computational domain. Intuitively, contribution of eigenstrains located near the boundaries of the computational domain might be truncated. Consequently, the accuracy of the predicted elastic fields might be affected. Therefore, numerical simulations are performed to validate the newly advanced algorithm.

2. PROBLEM DECOMPOSITION

As indicated by Chiu, [2], the influence coefficients can be obtained by decomposing the problem into three subproblems, as depicted in Fig. 1. The method consists in applying superposition principle to elastic states (b), (c), and (d), whose summation simulates the elastic state of the original problem (a). According to the principle of uniqueness of solutions in elastostatics, the found solution is the required one.

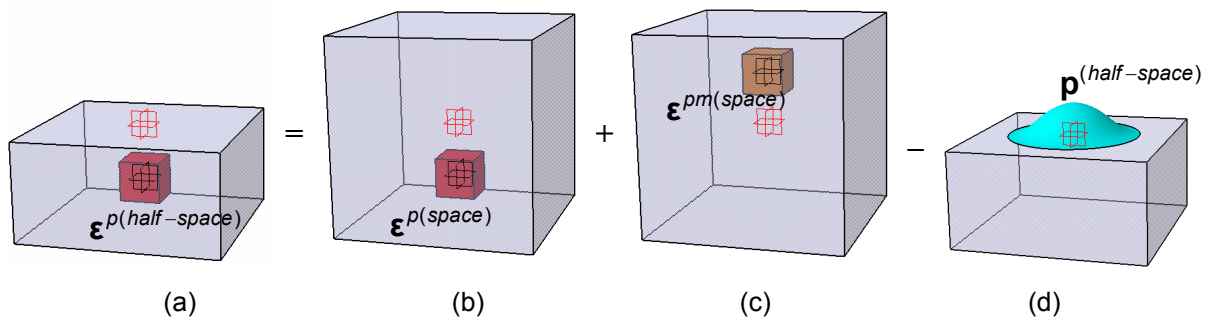


Figure 1. Inclusion problem decomposition: a. cuboidal inclusion in elastic half-space; b. cuboidal inclusion in infinite elastic space; c. an image counterpart in infinite space; d. a half-space with a pressure distribution

Eigenstrains in state (b) are identical to those of the original problem (a), while in state (c), the cuboid is the mirror image of the original one with respect to half-space boundary. Eigenstrains in state (c) are chosen such as superposition of solutions (b) and (c) yields the same stress state as (a), except for the half-space boundary, where a spurious pressure is induced. State (d) suggests that, in order to simulate the pressure-free boundary condition, solution to this subproblem should be extracted from summation of solutions corresponding to states (b) and (c).

A fast algorithm to compute elastic fields corresponding to states (b) and (c) was advanced in a companion paper. Based on this development, the spurious normal traction induced on the half-space boundary, \mathbf{p} , needed to solve the state (d) in Fig. 1, can be expressed:

$$\begin{aligned} p(x_1, x_2) = \sigma_{33}^{r(space)}(x_1, x_2, 0) = A_{33k\ell}(x_1 - x'_1, x_2 - x'_2, -x'_3) \varepsilon_{k\ell}^p(x'_1, x'_2, x'_3) + \\ + A_{33k\ell}(x_1 - x'_1, x_2 - x'_2, x'_3) \varepsilon_{k\ell}^{pm}(x'_1, x'_2, -x'_3), \end{aligned} \quad (1)$$

where (x_1, x_2, x_3) is the observation point and (x'_1, x'_2, x'_3) the source point (the control point of the cuboid). The influence coefficients $A_{33k\ell}$ can be expressed from Hooke's law, as suggested in [1]:

$$A_{3311} = \frac{\lambda}{8\pi^3} \sum_{m=1}^8 \left[\begin{aligned} & D_{,1111}(\mathbf{c}_m) + D_{,3333}(\mathbf{c}_m) + \frac{\nu}{1-\nu} D_{,2222}(\mathbf{c}_m) + \\ & + \frac{1}{1-\nu} (D_{,2233}(\mathbf{c}_m) + D_{,1122}(\mathbf{c}_m)) + \frac{-2\nu^2 + 4\nu - 1}{2\nu(1-\nu)} D_{,1133}(\mathbf{c}_m) \end{aligned} \right]; \quad (2)$$

$$A_{3322} = \frac{\lambda}{8\pi^3} \sum_{m=1}^8 \left[\begin{aligned} & D_{,2222}(\mathbf{c}_m) + D_{,3333}(\mathbf{c}_m) + \frac{\nu}{1-\nu} D_{,1111}(\mathbf{c}_m) + \\ & + \frac{1}{1-\nu} (D_{,1133}(\mathbf{c}_m) + D_{,1122}(\mathbf{c}_m)) + \frac{-2\nu^2 + 4\nu - 1}{2\nu(1-\nu)} D_{,2233}(\mathbf{c}_m) \end{aligned} \right]; \quad (3)$$

$$A_{3333} = \frac{\lambda}{4\pi^3} \sum_{m=1}^8 \left[\begin{aligned} & \frac{1-\nu}{\nu} D_{,3333}(\mathbf{c}_m) + \frac{\nu}{1-\nu} (D_{,1111}(\mathbf{c}_m) + D_{,2222}(\mathbf{c}_m)) + \\ & + \frac{2(1-\nu)}{\nu} (D_{,1133}(\mathbf{c}_m) + D_{,2233}(\mathbf{c}_m)) + \frac{2\nu}{1-\nu} D_{,1122}(\mathbf{c}_m) \end{aligned} \right]; \quad (4)$$

$$A_{3312} = \frac{\lambda}{4\pi^3} \sum_{m=1}^8 (1-2\nu) \left[\frac{D_{,1112}(\mathbf{c}_m) + D_{,1222}(\mathbf{c}_m)}{1-\nu} - \frac{D_{,3312}(\mathbf{c}_m)}{\nu} \right]; \quad (5)$$

$$A_{3323} = \frac{\lambda}{8\pi^3} \sum_{m=1}^8 \frac{2(1-2\nu)}{\nu(1-\nu)} [D_{,1123}(\mathbf{c}_m) + D_{,2223}(\mathbf{c}_m)]; \quad (6)$$

$$A_{3313} = \frac{\lambda}{8\pi^3} \sum_{m=1}^8 \frac{2(1-2\nu)}{\nu(1-\nu)} [D_{,2213}(\mathbf{c}_m) + D_{,1113}(\mathbf{c}_m)], \quad (7)$$

where μ and λ are Lamé's constants, \mathbf{c}_m , $m = \overline{1,8}$ are the eight vectors linking the corners of the cuboid to the observation point, and $D(\mathbf{c}_m)$ is a function whose fourth derivatives with respect to coordinates x'_j are obtained by circular permutation in one of four categories, $D_{,1111}$, $D_{,1112}$, $D_{,1122}$ and $D_{,1123}$, given in [1].

If an arbitrarily shaped inclusion is divided into multiple cuboids of uniform eigenstrains, after superimposing the individual contributions of all cuboids, Eq. (1) becomes:

$$\begin{aligned} p(x_1, x_2) = \sigma_{\xi\xi}^{r(space)}(i, j, 0) = & \sum_{\ell=1}^{N_1} \sum_{m=1}^{N_2} \sum_{n=1}^{N_3} A_{\xi\xi\zeta\zeta\gamma\gamma}(i-\ell, j-m, -n) \varepsilon_{\zeta\gamma}^p(\ell, m, n) + \\ & + \sum_{\ell=1}^{N_1} \sum_{m=1}^{N_2} \sum_{n=1}^{N_3} A_{\xi\xi\zeta\zeta\gamma\gamma}(i-\ell, j-m, n) \varepsilon_{\zeta\gamma}^p(\ell, m, n), \end{aligned} \quad (8)$$

where notation with respect to coordinates was substituted by notation with respect to indexes of elementary cells. As opposed to \mathbf{p} in Eq. (1), which expresses the effect of a single cuboid, Eq. (8) accounts for the contributions of all cuboids in the domain of analysis. The stress induced in the half-space can then be computed:

$$\sigma_{\xi\xi}^{(pressure)}(i, j, m) = \sum_{k=1}^{N_1} \sum_{\ell=1}^{N_2} Q_{\xi\xi}(i-k, j-\ell, m) p(k, \ell). \quad (9)$$

The product in Eq. (9) is a two-dimensional convolution with respect to directions of \bar{x}_1 and \bar{x}_2 . Finally, the solution for the stress due to arbitrarily shaped eigenstrains in an elastic isotropic half-space results from superposition of solutions (8) and (9), as depicted in Fig. 1.

3. ACCELERATION OF COMPUTATION

The following step is to compute the stress state induced in the half-space by \mathbf{p} . In existing formulations, [2-3], these stresses are expressed explicitly as functions of eigenstrains ε_{ij}^p . This rigorous formulation results in increased model complexity. It also has the disadvantage of limiting the application of spectral methods to two-dimensional case. However, if the analysis domain is large enough, one can assume that the normal traction induced on the half-space boundary vanishes outside the computational domain. Therefore, the corresponding elastic state is due to term $\sigma_{33}^{(0)}$ alone. With this assumption, computation of elastic state (d) is reduced to the problem of a stress state induced in an elastic isotropic half-space by an arbitrarily, yet known, pressure (or normal traction). Solution of this problem is readily available, as corresponding Green functions are known from Boussinesq fundamental solutions. The influence coefficients Q_{ij} result from

integration of Boussinesq formulas over elementary grid cell with respect to directions of \bar{x}_1 and \bar{x}_2 . The following primitives can be used:

$$q_{11}(x_1, x_2, x_3) = \frac{x_1 x_2 x_3}{r(x_1^2 + x_3^2)} + (1 - 2\nu) \left(\tan^{-1} \left(\frac{x_1}{x_2} \right) - \tan^{-1} \left(\frac{x_1 x_3}{x_2 r} \right) \right) - \tan^{-1} \left(\frac{x_1 x_2}{x_3 r} \right); \quad (10)$$

$$q_{22}(x_1, x_2, x_3) = q_{11}(x_2, x_1, x_3); \quad (11)$$

$$q_{33}(x_1, x_2, x_3) = -\tan^{-1} \left(\frac{x_1 x_2}{x_3 r} \right) - \frac{x_1 x_2 x_3 (r^2 + x_3^2)}{r(x_1^2 + x_3^2)(x_2^2 + x_3^2)}; \quad (12)$$

$$q_{12}(x_1, x_2, x_3) = (2\nu - 1) \log(r + x_3) - x_3/r; \quad (13)$$

$$q_{23}(x_1, x_2, x_3) = x_1 x_3^2 / [r(x_2^2 + x_3^2)]; \quad (14)$$

$$q_{31}(x_1, x_2, x_3) = q_{23}(x_2, x_1, x_3), \quad (15)$$

with $r = \sqrt{x_1^2 + x_2^2 + x_3^2}$.

Efficient computation of arising convolution products is available through Discrete Convolution Fast Fourier Transform (DCFFT) algorithm by Liu, Wang, and Liu, [4].

The resulting computational advantage is more effective when using the newly proposed algorithm as part of an elastic-plastic contact code, [8]. Indeed, influence coefficients Q_{ij} needed to assess stresses induced by arbitrarily pressure are shared with the elastic contact code. They are computed and stored as a $N_1 \times N_2 \times N_3$ array, with the aid of primitives (10) - (15). In Jacq's formulation, N_3 arrays of $N_1 \times N_2 \times N_3$ terms are needed, because the influence coefficients needed to impose free surface relief depend explicitly on both source and computation point depths. This double dependence also limit the use of spectral methods to two dimensions, thus being of order $O(N_3^2 N_1 N_2 \log N_1 N_2)$, [9]. In the simplified formulation advanced in this paper, as source domain (namely pressure domain) is only two-dimensional, as opposed to eigenstrains domain, which is three-dimensional, the computational order is decreased to $O(N_1 N_2 N_3 \log N_1 N_2)$ operations.

The method for imposing the pressure-free condition assumes that spurious normal tractions on the half-space boundary vanish outside computational domain. This assumption requires a larger computational domain in order to minimize truncation errors. When simulating concentrated elastic-plastic contacts, plastic region is usually located under the central region of the contact area, occupying a hemispherical domain. Therefore, the newly proposed method is well adapted to this kind of problems. As inclusion problem has to be solved repeatedly in an elastic-plastic contact simulation, the overall computational advantage is remarkable, allowing for finer grids or smaller loading steps to reduce discretization error.

4. PROGRAM VALIDATION

Using results presented by MacMillan, [6], Mindlin and Cheng, [7], derived the thermoelastic field due to a spherical inclusion in a half-space. Their analytical formulas were used as reference by Liu and Wang, [5], and also by Zhou, Chen, Keer, and Wang, [10]. These results are also used to validate the computer program advanced in this paper. To this end, a cuboidal domain, of elastic parameters ν and E and sides $L_1 = L_2 = L_3 = a$, is considered with a spherical inclusion of radius $R = 7/16 a$, centered at $(L_1/2, L_2/2, L_3/2)$. In this configuration, the computational domain exceeds the inclusion domain with only a

small amount. In most elastic-plastic contact problems, the computational domain is chosen to be much larger than the region with plastic strains.

Firstly, the inclusion is assumed to have uniform dilatational eigenstrains, $\varepsilon_{ij}^p = q\delta_{ij}$, with q a constant and δ_{ij} Kronecker's delta. Dimensionless stresses $\bar{\sigma}_{ij}^r = \sigma_{ij}^r / \sigma_0$ are defined as ratios to $\sigma_0 = Eq / (3(1-\nu))$, and dimensionless coordinates as ratios to corresponding cuboid sides: $\bar{x}_i = x_i / L_i$. A $96 \times 96 \times 96$ discretization was imposed in the computational domain.

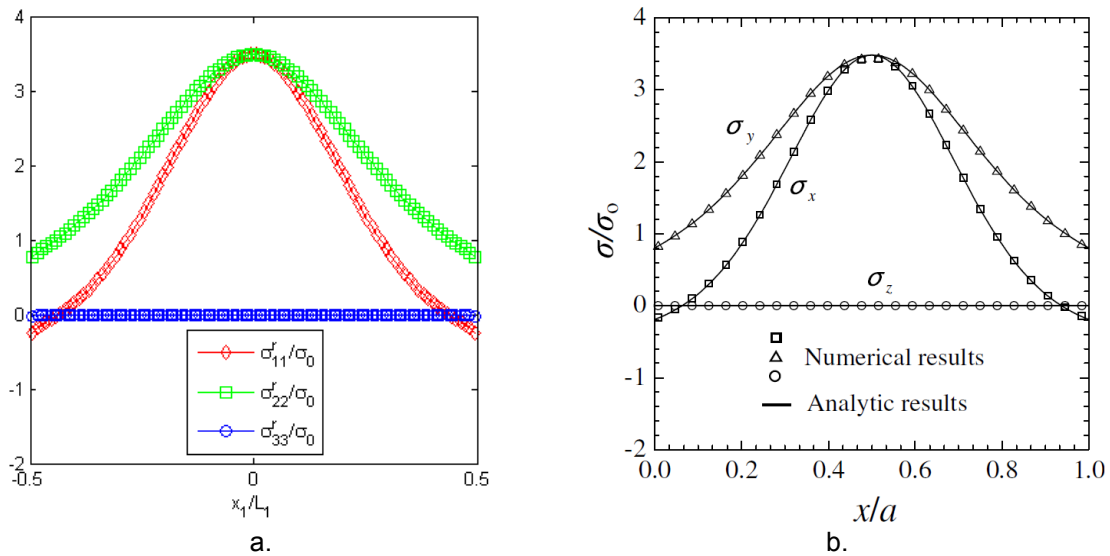


Figure 2. Normal stresses $\bar{\sigma}_{ij}^r$ along the x_1 -axis: a. this code; b. Zhou, Chen, Keer, and Wang, [10]

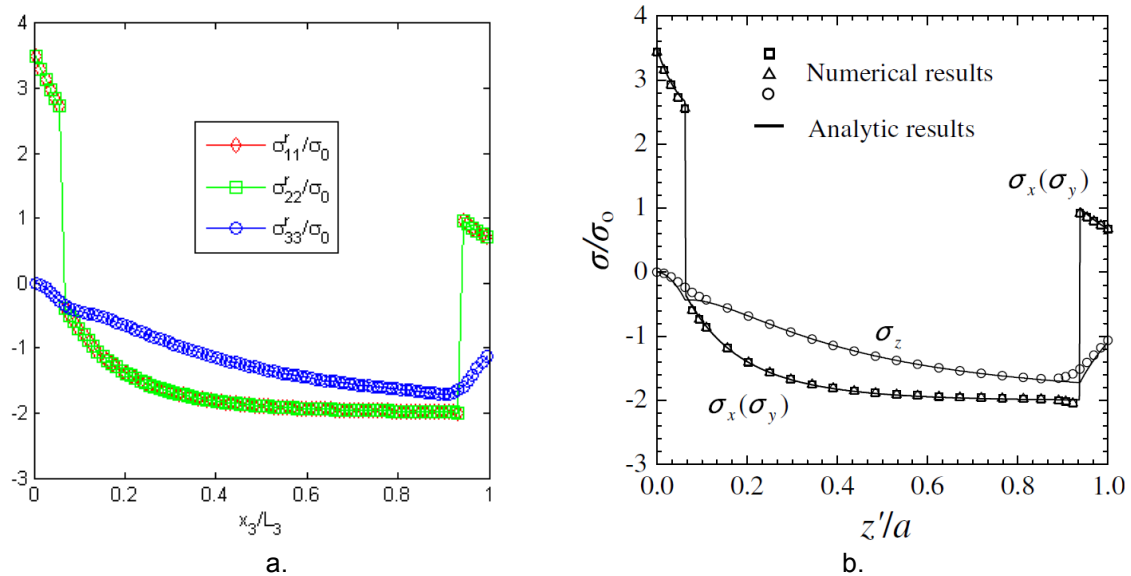


Figure 3. Normal stresses $\bar{\sigma}_{ij}^r$ along the x_3 -axis: a. this code; b. Zhou, Chen, Keer, and Wang, [10]

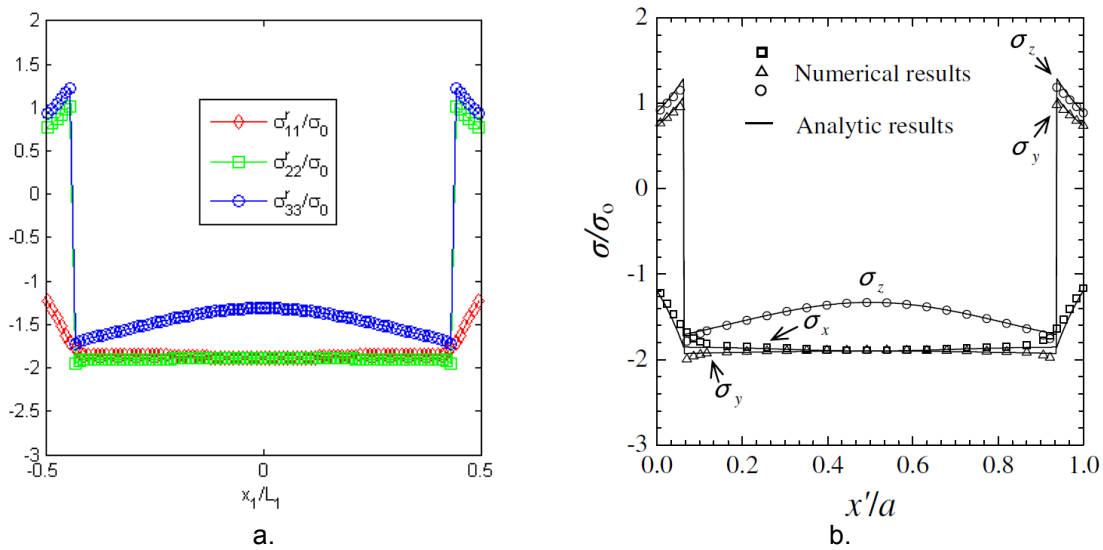


Figure 4. Normal stresses $\bar{\sigma}_{ij}^r$ along a horizontal axis passing through the center of the sphere: a. this code; b. Zhou, Chen, Keer, and Wang, [10]

The distribution of $\bar{\sigma}_{33}^r$ in Fig. 2 shows that normal tractions vanish on the half-space boundary, thus satisfying the pressure-free surface condition imposed in the algorithm. Stress distributions in Figs. 2.a – 4.a show a good match with analytical formulas advanced in [7] and with numerical predictions of Zhou, Chen, Keer, and Wang, [10], giving confidence in the newly proposed algorithm. The maximum errors compared to analytical formulas are located at the boundary of the spherical inclusion, and can be attributed to discretization error, namely to discretization of the sphere into cuboids, and not to problem decomposition. A fine resolution is required to capture the detailed behavior of the induced stresses at the spherical interface. However, this should be correlated with the available computational resources.

Liu and Wang, [5], present an extensive set of results, including the case when eigenstrains vary linearly with the distance from the center of the spherical inclusion. The algorithm described in [5] is based on a different approach, with no problem decomposition. In order to reproduce these results, a spherical inclusion of radius a is considered in a cuboid of sides $L_1 = L_2 = 4a$, $L_3 = 3a$. The center of the inclusion is located at depth Z_0 . Eigenstrains are assumed to vary proportional with the distance d from the center of the sphere:

$$\varepsilon_{ij}^p = (1 - d/a)q\delta_{ij}. \quad (16)$$

Distributions of $\bar{\sigma}_{33}^r$ along the x_3 - axis and in plane $x_2 = 0$, for different values of Z_0 , are depicted in Fig. 5. For this kind of inclusion, simulations predict that stress $\bar{\sigma}_{33}^r$ is almost linear inside the sphere.

All presented distributions reveal that numerical predictions obtained using the newly proposed algorithm agree well with analytical or numerical results already published. Consequently, the error introduced by truncation of normal tractions in infinite space partial solution can be considered as negligible for the type of inclusions investigated in this paper. Application to elastic-plastic non-conforming contact problems is therefore straightforward.

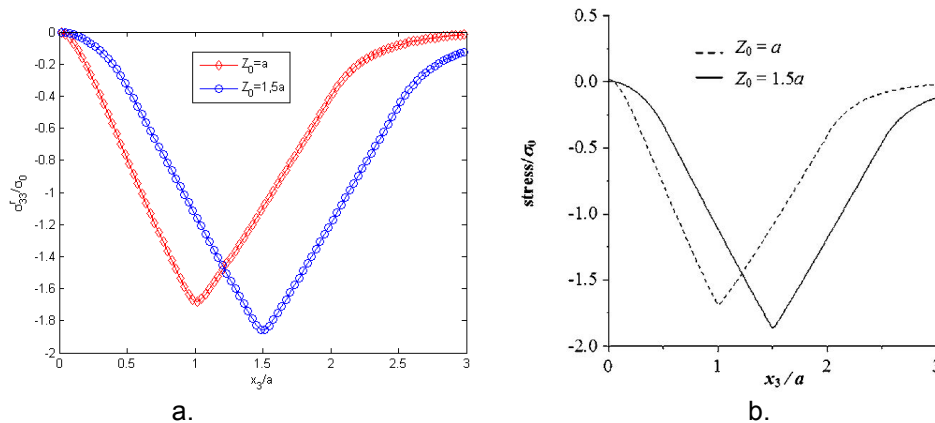


Figure 5. Dimensionless stress $\bar{\sigma}_{33}^r$ along the x_3 - axis, different Z_0 :
a. this code; b. Liu and Wang [5]

5. CONCLUSIONS

An algorithm for efficient computation of elastic fields due to arbitrarily shaped eigenstrains is validated in this paper by comparison with existing analytical and/or numerical results. This validation is required as the simplified method to impose the pressure-free surface condition in Chiu's inclusion problem decomposition implies truncation.

The computational advantage of the method yields from the efficiency of the algorithm for assessment of stress field in an elastic half-space due to an imposed pressure distribution. It requires only N_3 two dimensional DCFFT computations, as opposed to existing formulation, [9], in which N_3^2 two dimensional DCFFTs are needed.

Numerical predictions agree well with explicit formulas advanced by Mindlin and Cheng for a spherical inclusion of uniform eigenstrains. When eigenstrains are assumed proportional to distance from the center of the sphere, Liu and Wang's numerical results are used to benchmark the newly advanced algorithm. In all cases, a good agreement with existing results is found.

The newly proposed method is well adapted to elastic-plastic non-conforming contact simulation, and can be used to impose finer problem discretization, as shown in [8].

REFERENCES

- [1] Chiu, Y. P., (1977), *On the Stress Field Due to Initial Strains in a Cuboid Surrounded by an Infinite Elastic Space*. ASME J. Appl. Mech., 44, pp. 587–590.
- [2] Chiu, Y. P., (1978), *On the Stress Field and Surface Deformation in a Half Space with Cuboidal Zone in Which Initial Strains Are Uniform*. ASME J. Appl. Mech., 45, pp. 302–306.
- [3] Jacq, C., Nelias, D., Lormand, G., and Girodin, D., (2002), *Development of a Three-Dimensional Semi-Analytical Elastic-Plastic Contact Code*. ASME J. Tribol., 124, pp. 653–667.
- [4] Liu, S. B., Wang, Q., and Liu, G., (2000), *A Versatile Method of Discrete Convolution and FFT (DC-FFT) for Contact Analyses*. Wear, 243 (1–2), pp. 101–111.
- [5] Liu, S. Wang, Q., (2005), *Elastic Fields due to Eigenstrains in a Half-Space*. ASME J. Appl. Mech. 72, pp. 871–878.
- [6] MacMillan, W. D., (1930), *Theory of the Potential*. McGraw-Hill, New York.
- [7] Mindlin, R. D., and Cheng, D. H., (1950), *Thermoelastic Stress in the Semi-Infinite Solid*. J. Appl. Phys., 21, pp. 931 - 933.
- [8] Spinu, S., (2009), *Contributions to the Solution of the Elastic-Plastic Normal Contact Problem* (in Romanian). PhD Thesis, University of Suceava, Romania.
- [9] Wang, F., and Keer, L. M., (2005), *Numerical Simulation for Three Dimensional Elastic-Plastic Contact With Hardening Behavior*. ASME J. Tribol., 127, pp. 494–502.
- [10] Zhou, K., Chen, W. W., Keer, L. M., and Wang, Q. J., (2009), *A Fast Method for Solving Three-Dimensional Arbitrarily Shaped Inclusions in a Half-Space*. Comput. Methods Appl. Mech. Engrg, 198, pp. 885 - 892.